PV Hosting Capacity Assessment in Distribution Systems Considering Resilience Enhancement

Juan M. Home-Ortiz[1*], Ozy D. Melgar-Dominguez[1], José Roberto Sanches Mantovani[1], and João P. S. Catalão [2]

[1] Electrical Engineering Department, São Paulo State University (UNESP), Ilha Solteira, São Paulo, Brazil. (emails:{juanmanuelhome, ozzydamedo}@gmail.com, mant@dee.feis.unesp.br)

[2] Faculty of Engineering of the University of Porto and INESC TEC, Porto. Portugal (e-mail: catalao@fe.up.pt)

[*] Corresponding Author, Av. Brasil 056, UNESP - Campus de Ilha Solteira, Departamento de Engenharia Elétrica, Ilha Solteira, 15385000, São Paulo, Brazil. Tel: 3743-1000.

Abstract

This paper presents an innovative strategy to assess the photovoltaic (PV)-based distributed generation (DG) hosting capacity considering the operation under normal and emergency conditions of electrical distribution systems (EDSs). In the emergency condition, the proposed strategy aims to improve the recoverability of EDSs against a set of high-impact fault scenarios. This recoverability process is achieved by the optimal coordination of topology reconfiguration, islanding operation of dispatchable DG units, and pre-positioning and displacement of mobile DG (MDG) units. This problem is formulated as a two-stage stochastic formulation, where the first one defines the DG hosting capacity and the amount of MDG units to be positioned in staging locations. Meanwhile, the second stage simulates high-impact fault events and, by applying resilience alternatives, the EDS recoverability can be improved. Inherently, the two-stage stochastic formulation is represented by a mixed-integer linear programming (MILP) model. The objective function of this MILP model maximizes the installed PV-based DG capacity while the amount of energy load shedding after fault events is minimized. To validate and show the scalability of the proposed strategy, two EDS are studied under different high-impact fault events and considering the application of multiple resilience alternatives. Results show that by estimating the capacity of PV-based DG simultaneously with the restoration process, the number of pre-positioned and dispatched MDG units can be reduced. On the other hand, when this PV capacity is determined disregarding fault scenarios, this solution could lead to unviable conditions and, thus, generation curtailment of up to 80% could be required.

Keywords: Islanding operation, mobile distributed generation units, PV hosting capacity, resilience enhancement.

Nomenclature

Sets and indexes

Γ_G/Γ_{SS} Set of buses with dispatchable DG / substation

Γ_B/Γ_N Set of lines / buses of the system

$\Gamma_N^{mdg}/\Gamma_{st}$ Set of connection buses for MDG / staging location

$\Gamma_C^t/\Gamma_T/\Gamma_F$ Set of stochastic scenarios/ time period/ fault events

$\Gamma_{\overline{n}}^{mdg}$ Set of maximum MDG units to be pre-positioned

Γ_B^* Set with indexes ij and ji of each line of the system, including the fictitious grid

Γ_B^F Set of fictitious lines that connect the fictitious substation to each node of the system

Γ_N^f Set of buses that were not affected by a fault scenario f

$c/t/f$ Index of scenario / time period / fault scenario

$i, j/st$ Index of buses / staging locations

ij/ji Indexes of lines

Parameters

Δ_t/σ_i Duration of a time period / Load shedding cost

$\rho_{t,c}$ Probability of stochastic scenario

$\xi_{i,t,c}$ PV generation level at bus i, time t, scenario c

C_i^t Required time to connect a MDG unit to the bus i

P^d/Q^d Active/reactive power demand

R_{ij}/X_{ij} Resistance/reactance of line ij

$\overline{S}_i^{dg}/\overline{S}_i^{ss}$ Apparent power limit of DG / substation

$\overline{S}_{ij}$ Apparent power limit of a line

$T^{cf}_{st,i}$ Time considered to be affected by the road congestion between staging location st and bus i

$T^{t}_{st,i}$ Traveling time between staging location st and bus i

$\overline{V}$, $\underline{V}$ Maximum/minimum voltage limits

$\hat{y}_{ij}$ Initial state of line ij

Binary variables

$F^{G}_{ij,f}$ Auxiliary binary variable for the operational state of the lines with the DG units as reference

$F^{SS}_{ij,f}$ Auxiliary binary variable for the operational state of the lines with the substation as reference

$k^{mdg}_{st,n}$ Binary variable that defines the pre-positioned n MDG units at location st

$u_{i,n,t,f}$ Binary variable that defines the n MDG units connected at bus i, time t, fault f

$w_{i,n,t,f}$ Binary variable that defines the connection time t of a MDG unit at bus i, fault f

$y_{ij,f}/x_{i,f}$ Binary variable for operational state of lines /buses

$z^{mdg}_{st,i,n,f}$ Binary variable that indicates the displacement of n MDG units from st to i, fault f

Continuous variables

$P^{curt}_{i,t,c}$ PV power curtailment at bus i, time t, and scenario c

P^{ins}_{i} PV installed capacity at bus i

$P^{dg/ss}_{i,t,c}$ Post-fault active power injected by DG / substation.

$P_{ij,t,c}$ Post-fault active power flow through a line.

$P^{mdg/pv}_{i,t,c}$ Active power injected by a MDG / PV unit.

$\hat{P}^{dg/ss}_{i,t,c}$ Pre-fault active power injected by DG / substation.

$\hat{P}_{ij,t,c}$ Pre-fault active power flow through a line.

$Q^{dg/ss}_{i,t,c}$ Post-fault reactive power injected by DG / substation.

$Q^{mdg/pv}_{i,t,c}$ Reactive power injected by a MDG / PV unit.

$Q_{ij,t,c}$ Post-fault reactive power flow through a line.

$\hat{Q}^{dg/ss}_{i,t,c}$ Pre-fault reactive power injected by DG / substation.

$\hat{Q}_{ij,t,c}$ Pre-fault reactive power flow through a line.

$T^{x}_{st,i,n,f}$ Traveling time by n MDG units from st to i, fault f

$V^{sqr}_{i,t,c}$ Post-fault square of the voltage.

$\hat{V}^{sqr}_{i,t,c}$ Pre-fault square of the voltage at a node.

1. Introduction

Extreme and rare incidents such as natural disasters, technical problems, and cyber-attacks can trigger power outages in electric distribution systems (EDSs). Under this scenario, distribution system operators (DSOs) have the responsibility for efficiently developing their EDSs and apply some procedures to obtain a capable EDS to quickly recover to an acceptable operating state, guaranteeing to passive and active users a continuous and secure power service. This condition gives rise to the concept of resilience, defined as the capability of the system to anticipate, recover, and deal with extreme and rare incidents [1] changing the philosophy of traditional expansion and operation planning to design resilient EDSs [2].

Naturally, the challenge of planning a more resilient EDS is increased with the liberalization of electricity markets, where the DSO should provide network access to all new distributed generation (DG) connection requests. In this regard, it is necessary to assess the capacity of the current EDS infrastructure to accommodate high shares of DG, without negatively impacting on the EDS operation [3]. Until now and considering only normal operation conditions, some strategies have been developed to explore both the coordination of operational resources that exploit the EDS infrastructure [4] and the implementation of actions to upgrade the network infrastructure from distribution systems [5] to transmission level [6]. Therefore, the DSO should develop more robust strategies capable of dealing with the complexities of estimating the maximum DG capacity that can be accommodated in an EDS under the perspective of resilient systems.

1.1. Literature review

From different perspectives, several studies have been presented with the primary goal of enhancing the resilience of EDSs [7]. The resilience problem can be approached through strategies of infrastructure hardening or with the implementation of operational procedures [8]. Infrastructure-hardening strategies require some investment actions to strengthen the EDS against the worst operating condition [9]. For example, in the literature can be found strategies based on the allocation of mobile and fixed distributed generation (DG)

units [10], the allocation of dispatchable DG units and the optimal formation of microgrids (MGs) through topology reconfiguration [11], multi-disaster-scenarios for power lines hardening and back-up DG units [12], hardening plans to minimize costs of repair, operation and load shedding [13].

On the other hand, some works are based on operational strategies for dealing with emergency conditions in EDSs. In this research field, a method for mitigating negative effects during emergency conditions is presented in [14]. In this approach, the on-outage area was sectionalized into MGs, and the power dispatch of existing DG units re-dispatched to supply affected users. In the same way, the authors in [15] propose an approach to deal with fault events by considering the MGs formation and by applying a master-slave operation of DG units. *Chen et al.* [16] propose a methodology for service restoration by optimizing the coordination of controllable switches, energy storage systems (ESSs), and dispatchable DG units. To overcome an emergency condition after the occurrence of a disaster, an approach for restoring the power service is presented in [17]. This strategy co-optimizes the operation of mobile DG (MDG) units and repair crews to restore the EDS via the dynamic formation of MGs. As a response to improve the resilience of EDSs in facing high impact disruptions, a multi-decision methodology is proposed by the authors in [18]. This methodology employs some switching actions for remote-control and manual switches while crews and MDG units are pre-positioned to speed up the post-disturbance actions.

Nowadays, the necessity of accommodating high shares of renewable-based DG has been a concern for the DSOs, who seek at estimating the maximum DG capacity that can be accommodated in an EDS, encouraging the participation of new investors. This capacity can be determined through a hosting capacity analysis and, leveraging the current EDS infrastructure, the coordinated application of active network management schemes to maximize that capacity can be explored, as presented in [19]. This strategy coordinates the operation of voltage regulators and adjusts the DG power factor and generation curtailment to enable a greater DG penetration level. A probabilistic bilevel approach is presented in [20], where it maximizes the DG penetration by taking advantage of the network reconfiguration. Reference [21] proposes a method for the optimal coordination of ESSs with the goal of estimating the wind and photovoltaic (PV)- based DG hosting capacity in EDSs. To take advantage of the complementary of wind and PV technologies, the authors in [22] develop a study to evaluate, from a probabilistic perspective, the DG hosting capacity of hybrid systems. In [23], the DG hosting capacity is maximized by optimal coordination of Volt/Var devices, where it is modeled the effects of voltage-dependent loads for establishing the relationship of demand consumption and renewable energy production.

Other network flexibilities to increase the DG hosting capacity were explored in [24], where the optimal coordination of DG power factor, OLTC tap changers, and network reconfiguration are simultaneously opti-

mized. The application of other technologies has been studied in this research field; for example, reference [25] formulates an approach that leverages controllable features of electric vehicles for increasing the DG hosting capacity in EDSs. A probabilistic hosting capacity analysis of harmonic-distorted distribution system is explored in [26], where a passive harmonic filter is proposed to maximize the DG hosting capacity. In [27], it is presented a two-stage strategy to improve the grid-connected MG performance, where the ESS allocation is carried out to enhance the self-consumption and the hosting capacity of renewable sources in a MG. The authors in [28] enhance the DG penetration through a sequential network reconfiguration and the placement of soft open points. It is important to note that the DG hosting capacity has been evaluated through multi-periods representations that typically capture the EDS operation only on normal operating conditions.

1.2. Research Gap and Novel Contributions

Although an adequate number of approaches are available in the literature to estimate the DG hosting capacity in EDSs, still there are several challenges that need to be incorporated to consider the implications of emergency conditions due to high-impact fault events. As evidenced in the literature, the DG hosting capacity problem in EDSs has been focused only on normal operational conditions, where strategies to deal with emergency conditions due to disasters have been disregarded. Motivated by the previous review, this work aims to fill the void existing in the literature through a novel strategy to assess the PV-based DG hosting capacity under normal and emergency conditions. The problem is methodologically designed as a two-stage stochastic formulation, where the first stage, denoted as the planning problem, defines the maximum amount of DG to be connected to the EDS, and the amount of MDG units to be positioned. Meanwhile, the second stage simulates the system operation reaction due to first-stage decisions and considering normal and emergency conditions.

The proposed formulation characterizes uncertainties of demand and DG power production by using a finite number of scenarios obtained from historical data. Meanwhile, the problem is approximated to a mixed-integer linear programming (MILP) model. Therefore, the solution of this model defines the maximum PV-based DG capacity to be connected to an EDSs, this capacity is assessed under normal and emergency conditions, where in the latter condition several operational resources should be implemented to improve the EDS recoverability. Table 1 illustrates the main differences of the proposed approach compared to the existing methodologies to improve the recoverability in EDSs. In this table, symbols "✓" and "×" indicate whether a particular task has been addressed or not.

Based on the exhaustive literature review, the contributions of the presented work are classified as follows:

Table 1: Taxonomy of relevant works in the area

Ref.	Hosting capacity	MEG	Islanding operation	Restoration
[6]	×	✓	✓	✓
[7]	×	×	✓	✓
[8]	×	×	✓	✓
[10]	×	×	✓	×
[11]	×	×	✓	✓
[12]	×	×	×	✓
[13]	×	✓	✓	✓
[14]	×	✓	✓	✓
Proposed approach	✓	✓	✓	✓

- Proposing an innovative strategy that assesses the PV-based DG hosting capacity under normal and emergency conditions. The strategy is designed to simultaneously deal with planning and operation decisions under the uncertainty behavior of demand and PV-based power production via a stochastic multiperiod and multi-stage formulation. The first stage, denoted as the planning stage, defines the maximum amount of PV-based DG connected to an EDS and reinforces it by placing the MDG units at staging locations to deal with emergency conditions. The operating reaction, due to the first-stage decisions and high-impact fault events, is accounted in the second stage, where it coordinates the optimal operation of resources such as network reconfiguration, islanding DG operation, reactive power dispatch of DG units, and dispatching and operation of MDG units.

- Proposing a MILP model for representing, in a suitable way, the PV-based DG hosting capacity problem considering the EDS resilience enhancement. The solution of this model defines several actions (in planning and operation stages) that provide a comprehensive picture of the evaluation of the effects of high-impact fault events on the estimation of the DG penetration level that should be connected to an EDS. Therefore, the proposed strategy is provided as an effective tool to assist the DSO in the decision-making process to develop more resilient EDSs considering the integration of high shares of renewable-based DG.

This work is structured as follows: Section II presents in detail the mathematical formulation of the problem; Section III presents study cases under diffeten test conditions to evaluate the performance of the proposed strategy and also presents the obtained results and discussion for two test EDSs; finally, conclusions are drawn in Section IV.

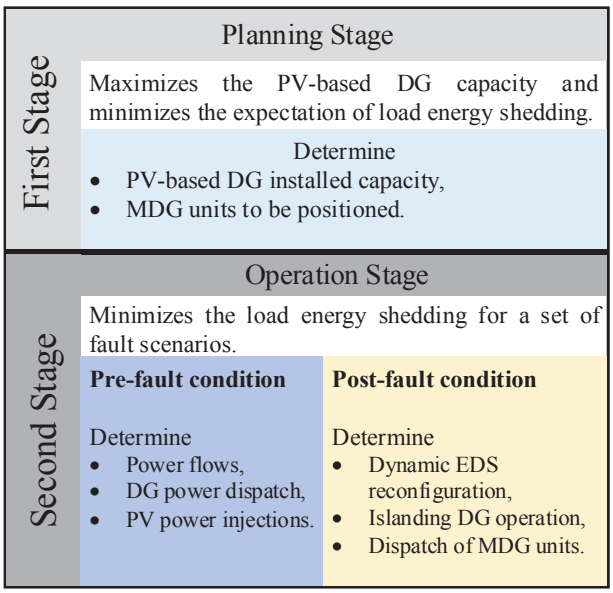

Figure 1: Two-stage structure of the stochastic MILP problem

2. Problem Formulation

The DG hosting capacity assessment corresponds to a planning problem, where it is estimated the maximum amount of DG to be accommodated to an EDS considering a planning horizon of years. In this work, a planning horizon of one year is adopted, where it is characterized by representative time intervals to capture the variability of demand and generation, and operational characteristics of an EDS under normal and emergency conditions. These conditions, denoted by pre- and post-fault conditions, are simulated to apply some alternatives to improve the EDS resilience after extreme incidents. The DG hosting capacity problem under such circumstances is tackled as a two-stage stochastic approach illustrated in Fig. 1, where each stage is defined as follows:

- The first stage problem seeks to estimate the maximum amount of PV-based DG that can be accommodated to an EDS and minimizes the expectation of the EDS load energy shedding (obtained from the second stage problem) evaluated on all uncertainties and fault scenarios. This stage should define the installed DG capacity at each predefined bus, and the MDG units to be positioned at predefined staging locations in order to deal with emergency conditions.

- Once estimated, in the first stage problem, the maximum DG capacity to be accommodated and defined the number of MDG units to be positioned, the second stage evaluates the operating reaction of the EDS considering normal and emergency conditions due to high-impact fault events. For each fault scenario, operational resources such as the dynamic EDS reconfiguration, the islanding operation of

dispatchable DG units, and the dispatch of MDG units are coordinated to minimize the load energy shedding.

To solve this two-stage stochastic problem, uncertainties in demand consumption and DG power production are represented by a finite number of scenarios that can be generated using probability density functions or historical data. This standard approach allows to recast the original problem as a single-level MILP model, for which classical optimization techniques can be used to determine its solution [29].

Therefore, this section presents the mathematical formulation of the MILP model. This formulation is classified by pre- and post- fault EDS operation, equations of network reconfiguration, pre-location and scheduling of MDG units, islanding operation of DG units, and hosting capacity of PV-based DG.

2.1. Objective function

The mathematical formulation is a two-stage stochastic scenario-based model that aims to attend simultaneously pre- and post-emergency conditions. The proposed objective function (1) maximizes, for the planning horizon, the total PV-based DG installed capacity (first term) of the system while simultaneously minimizes the expected load energy shedding of the EDS (second term) for a set of possible fault scenarios.

$$\max \sum_{i\in\Gamma_{PV}} P_i^{ins} - \sum_{t\in\Gamma_T}\sum_{c\in\Gamma_C^t}\sum_{f\in\Gamma_F}\left[\rho_{t,c,f}\sum_{i\in\Gamma_N}\sigma_i\Delta_t\sqrt{(P_{i,t,c}^d)^2+(Q_{i,t,c}^d)^2}x_{i,f}\right] \tag{1}$$

In the proposed formulation, for each fault scenario f, the binary variable $x_{i,f}$, that affects the second term in (1), determines if the load at node i is energized, then ($x_{i,f}=0$) and it does not affect the maximization of the objective function, otherwise if the load at node i is out-of-service then ($x_{i,f}=1$) and it is penalized in the objective function. In this regard, this term in the objective function aims to increase the energized load of the system. Note that, the load shedding cost σ_i can be used as a weighting parameter to determine priority loads, making nodes with higher σ_i values more attractive to be restored.

2.2. Pre-fault distribution system operation

The pre-fault steady-state operating point of an EDS is represented by the set of constraints (2)-(4).

$$\sum_{ji\in\Gamma_B}\hat{P}_{ji,t,c} - \sum_{ij\in\Gamma_B}\hat{P}_{ij,t,c} + \hat{P}_{i,t,c}^{ss} + P_{i,t,c}^{pv} + \hat{P}_{i,t,c}^{gd} = P_{i,t,c}^d, \qquad \forall(i,t,c), \tag{2}$$

$$\sum_{ji\in\Gamma_B}\hat{Q}_{ji,t,c}-\sum_{ij\in\Gamma_B}\hat{Q}_{ij,t,c}+\hat{Q}^{ss}_{i,t,c}+Q^{pv}_{i,t,c}+\hat{Q}^{gd}_{i,t,c}=Q^{d}_{i,t,c},\qquad \forall(i,t,c), \tag{3}$$

$$\hat{V}^{sqr}_{i,t,c}-\hat{V}^{sqr}_{j,t,c}=2(R_{ij}\hat{P}_{ij,t,c}+X_{ij}\hat{Q}_{ij,t,c}),\qquad \forall(ij,t,c|_{\hat{y}_{ij}=1}). \tag{4}$$

where the indices i, ij, t, c correspond to the sets $\Gamma_N, \Gamma_B, \Gamma_T, \Gamma^t_C$, respectively.

The active and reactive power flow balance is represented by (2) and (3), respectively. These expressions consider active and reactive power injection at node i by the substation, PV-based DG units, and dispatchable DG to attend the power demand. The square voltage drop is determined by (4), for in-service lines ($\hat{y}_{ij}=1$), this constraint is based on the DistFlow model proposed by [30].

$$(\hat{P}^{ss}_{i,t,c})^2+(\hat{Q}^{ss}_{i,t,c})^2\leq(\overline{S}^{ss}_{i})^2,\qquad \forall(i\in\Gamma_{SS},t,c), \tag{5}$$

$$(\hat{P}^{dg}_{i,t,c})^2+(\hat{Q}^{dg}_{i,t,c})^2\leq(\overline{S}^{dg}_{i})^2,\qquad \forall(i\in\Gamma_{G},t,c), \tag{6}$$

$$\hat{P}^{dg}_{i,t,c}\geq 0,\qquad \forall(i\in\Gamma_{G},t,c), \tag{7}$$

$$\hat{P}^{dg}_{i,t,c}\psi^{dg}_{cap}\leq\hat{Q}^{dg}_{i,t,c}\leq\hat{P}^{dg}_{i,t,c}\psi^{dg}_{ind},\qquad \forall(i\in\Gamma_{G},t,c), \tag{8}$$

$$\underline{V}^2\leq\hat{V}^{sqr}_{i,t,c}\leq\overline{V}^2,\qquad \forall(i\in\Gamma_{N},t,c), \tag{9}$$

$$(\hat{P}_{ij,t,c})^2+(\hat{Q}_{ij,t,c})^2\leq(\overline{S}_{ij})^2\hat{y}_{ij},\qquad \forall(ij\in\Gamma_{B},t,c). \tag{10}$$

Operational limits of substation, dispatchable DG units, and voltage and thermal limits are defined in (5)-(10). The capacity of the substation is defined by (5), where supllied active and reactive power are bounded by the apparent power. In the same way, the active and reactive power supplied by installed dispatchable DG units is limited by the DG capacity in (6). Constraint (7) defines the non-negativity of the variable that represents the active power supplied by dispatchable DG. The reactive power is controlled by a predefined power factor and the active power supplied by the DG in (8). The voltage magnitude at node i is bounded by (9) while thermal capacity of conductors is limited by (10).

2.3. DG Hosting Capacity

The DG hosting capacity problem is a crucial analysis for determining the maximum DG penetration level that an EDS can accommodate without violations of operational limits. From the DSO perspective, this practice resulted in developing innovative strategies for the planning and operation of EDSs. The proposed approach seeks to estimate this DG penetration level considering pre- and post- disturbance operating conditions. Expressions (11)-(14) are used to model the operation for each DG unit and to determine its maximum installed capacity. Note that, these DG units must be integrated into the EDS without operational

violations under pre-fault and post-fault emergency conditions; hence, these expressions are not affected by the fault scenarios.

$$P^{pv}_{i,t,c} = \xi_{i,t,c} P^{ins}_{i} - P^{curt}_{i,t,c}, \qquad \forall (i,t,c), \tag{11}$$

$$P^{curt}_{i,t,c} \leq \xi_{i,t,c} P^{ins}_{i}, \qquad \forall (i,t,c), \tag{12}$$

$$\sum_{t \in \Gamma T} \sum_{c \in \Gamma^{t}_{C}} P^{curt}_{i,t,c} \leq \gamma \sum_{t \in \Gamma_{T}} \sum_{c \in \Gamma^{t}_{C}} \xi_{i,t,c} P^{ins}_{i}, \qquad \forall (i), \tag{13}$$

$$P^{pv}_{i,t,c} \psi^{pv}_{cap} \leq Q^{pv}_{i,t,c} \leq P^{pv}_{i,t,c} \psi^{pv}_{ind}, \qquad \forall (i,t,c). \tag{14}$$

where the indices i, t, s correspond to the sets $\Gamma_N, \Gamma_T, \Gamma^t_C$, respectively.

The power injected by the renewable-based DG units is defined by (11). This power is defined as the product between the generation level (ξ) and the installed capacity (P^{ins}) minus the curtailed power (P^{curt}). Constraint (12) bounds the curtailed power to be less than the available power (ξP^{ins}). The maximum curtailment, defined for each PV unit, is set to a maximum percentage (γ) of the available generation using (13). Finally, the reactive power is controlled in (14) by using a predefined power factor ($\psi^{pv}_{cap}/\psi^{pv}_{ind}$) and the active power production ($P^{pv}_{i,t,c}$). Note that, this is a general formulation that can be extended to other generation technologies.

2.4. Pre-positioning stage of Mobile DG units

The MDG units can play an important role to restore loads under emergency situations. The dispatch problem of MDG units consists in allocating them in staging locations (st) and, when a fault event occurs, the MDG units must travel to be connected in appropriate buses with the aim of supplying affected loads as quickly as possible. Therefore, this problem is formulated considering two-stage defined as the pre-positioning stage and post-fault event stage. Prior to the occurrence of a fault event, emergency MDG units should be placed in the best available st. The amount of MDG units to be positioned in the EDS is limited by a maximum predefined value $\overline{K}_{st}$ in (15). The sequence of each MDG unit to be positioned in each st is defined by the logical constraint (16).

$$\sum_{n \in \Gamma^{mdg}_{\overline{n}}} k^{mdg}_{st,n} \leq \overline{K}_{st}, \qquad \forall st, \tag{15}$$

$$k^{mdg}_{st,n} \leq k^{mdg}_{st,n-1}, \qquad \forall (st,n). \tag{16}$$

2.5. Post-Fault Distribution System Operation

For each fault scenario $f \in \Gamma_F$, the steady-state condition of an EDS is determined by the set of constraints (17)-(20).

$$\sum_{ji\in\Gamma_B} P_{ji,t,c,f} - \sum_{ij\in\Gamma_B} P_{ij,t,c,f} + P^{ss}_{i,t,c,f} + P^{pv}_{i,t,c,f} + P^{dg}_{i,t,c,f} + P^{mdg}_{i,t,c,f} = P^{d}_{i,t,c}(1 - x_{i,f}), \qquad \forall(i,t,c,f), \qquad (17)$$

$$\sum_{ji\in\Gamma_B} Q_{ji,t,c,f} - \sum_{ij\in\Gamma_B} Q_{ij,t,c,f} + Q^{ss}_{i,t,c,f} + Q^{pv}_{i,t,c,f} + Q^{mdg}_{i,t,c,f} + Q^{dg}_{i,t,c,f} = Q^{d}_{i,t,c}(1 - x_{i,f}), \qquad \forall(i,t,c,f), \qquad (18)$$

$$V^{sqr}_{i,t,c,f} - V^{sqr}_{j,t,c,f} + v_{ij,t,c,f} = 2(R_{ij}P_{ij,t,c,f} + X_{ij}Q_{ij,t,c,f}), \qquad \forall(ij,t,c,f), \qquad (19)$$

$$-(\overline{V}^2 - \underline{V}^2)(1 - y_{ij,f}) \le v_{ij,t,c,f} \le (\overline{V}^2 - \underline{V}^2)(1 - y_{ij,f}), \qquad \forall(ij,t,c,f). \qquad (20)$$

where the indices i, ij, t, c, f correspond to the sets $\Gamma_N, \Gamma_B, \Gamma_T, \Gamma^t_C, \Gamma_F$, respectively.

Under emergency conditions, constraints (2)-(4) are recast to consider the occurrence of any fault-scenario. In contrast to (4), the voltage drop, defined by (20), is determined according to the operational state of circuit ij, where the slack variable $v_{ij,t,c,f}$ is used. When the operational state of circuit ij is open ($y_{ij,f} = 0$) then $v_{ij,t,c,f}$ is limited according to (20), otherwise $v_{ij,t,c,f}$ is equal to zero.

$$(P^{ss}_{i,t,c,f})^2 + (Q^{ss}_{i,t,c,f})^2 \le (\overline{S}^{ss}_i)^2, \qquad \forall(i \in \Gamma_{SS}, t, c, f), \qquad (21)$$

$$(P^{dg}_{i,t,c,f})^2 + (Q^{dg}_{i,t,c,f})^2 \le (\overline{S}^{dg}_i)^2(1 - x_{i,f}), \qquad \forall(i \in \Gamma_G, t, c, f), \qquad (22)$$

$$(P^{dg}_{i,t,c,f}) \ge 0, \qquad \forall(i \in \Gamma_G, t, c, f), \qquad (23)$$

$$P^{dg}_{i,t,c,f}\psi^{dg}_{cap} \le Q^{dg}_{i,t,c,f} \le P^{dg}_{i,t,c,f}\psi^{dg}_{ind}, \qquad \forall(i \in \Gamma_G, t, c, f), \qquad (24)$$

$$\underline{V}^2 \le V^{sqr}_{i,t,c,f} \le \overline{V}^2, \qquad \forall(i \in \Gamma_N, t, c, f), \qquad (25)$$

$$(P_{ij,t,c,f})^2 + (Q_{ij,t,c,f})^2 \le (\overline{S}_{ij})^2 y_{ij,f}, \qquad \forall(ij \in \Gamma_B, t, c, f). \qquad (26)$$

where the indices t, c, f correspond to the sets $\Gamma_T, \Gamma^t_C, \Gamma_F$, respectively.

In analogous way, operational limits of substation, dispatchable DG units, voltage and thermal limits are recast to cope with any fault event in (21)-(26). It worth noting that a dispatchable DG unit only can supply energy if it is installed in an in-service node. Thereby, the power injection of DG units depend on the state of the binary variable $x_{i,f}$. In order to reduce the computational effort, quadratic terms from equations (5), (6), (10), (21), (22), and (26) are approximated using piecewise linear functions as presented in [31].

2.5.1. Dispatch Problem of MDG units and Islanding Operation

In the proposed resilience-based strategy, alternatives as dispatching and optimal operation of MDG units, and islanding operation are taken into account for minimizing service interruption. This formulation is explained in this subsection.

2.5.2. Operation of MDG units in post-fault event stage

Under emergency conditions, the pre-positioned MDG units [first stage decision, see section 2.4] are dispatched to improve the recoverability of the EDS. Based on the formulation presented in [32], this dispatch problem is presented in (27)-(35).

$$\sum_{i\in\Gamma_N^{mdg}}\sum_{n\in\Gamma_{\overline{n}}^{mdg}} z_{st,i,n,f}^{mdg} \leq \sum_{n\in\Gamma_{\overline{n}}^{mdg}} k_{st,n}^{mdg}, \qquad \forall(st,f), \tag{27}$$

$$z_{st,i,n,f}^{mdg} \leq z_{st,i,n-1,f}^{mdg}, \qquad \forall(st,i,n,f), \tag{28}$$

$$T_{st,i,n,f}^{x} = (T_{st,i}^{cf} T_{st,i}^{t} + C_i^t) z_{st,i,n,f}^{mdg}, \qquad \forall(st,i,n,f), \tag{29}$$

$$\sum_{t\in\Gamma_T} tw_{i,n,t,f} \geq \sum_{st\in\Gamma_{st}} T_{st,i,n,f}^{x}, \qquad \forall(i,n,f), \tag{30}$$

$$\sum_{t\in\Gamma_T} tw_{i,n,t,f} \leq \sum_{st\in\Gamma_{st}} T_{st,i,n,f}^{x}, \qquad \forall(i,n,f), \tag{31}$$

$$\sum_{t\in\Gamma_T} w_{i,n,t,f} = \sum_{st\in\Gamma_{st}} z_{st,i,n,f}^{mdg}, \qquad \forall(i,n,f), \tag{32}$$

$$u_{i,n,t',f} = \sum_{t\in\Gamma_T} w_{i,n,t,f}, \qquad \forall(i,n,f,t' : t < t'), \tag{33}$$

$$0 \leq P_{i,t,c,f}^{mdg} \leq \overline{P}^{mdg} \sum_{n\in\Gamma_{\overline{n}}^{mdg}} u_{i,n,t,f}, \qquad \forall(i,n,t,c,f), \tag{34}$$

$$P_{i,t,c,f}^{mdg} \psi_{cap}^{mdg} \leq Q_{i,t,c,f}^{mdg} \leq P_{i,t,c,f}^{mdg} \psi_{ind}^{mdg}, \qquad \forall(i,t,c,f), \tag{35}$$

where the indices st, t, c, n, i, f correspond to the sets $\Gamma_{st}, \Gamma_T, \Gamma_C^t, \Gamma_{\overline{n}}^{mdg}, \Gamma_N^{mdg}, \Gamma_F$, respectively.

When a fault occurs, the DSO can send MDG units from the location st, where these units were pre-positioned, to the new position i. Expression (27) guarantees that the MDG units sent to the new locations i can not exceed the number of pre-positioned units, while the sequence of each unit sent to i is defined by (28). The travel time (T^x) requested by each MDG unit from st to i is determined by (29). This time is defined as the traveling time between two points (T^t), st and i plus the required time to connect (C_i^t) the MDG unit to the bus i. To deal with the traffic congestion, a road congestion time factor (T^{cf}) is added in the formulation, affecting the traveling time. The determined travel time is used in expressions (30) and

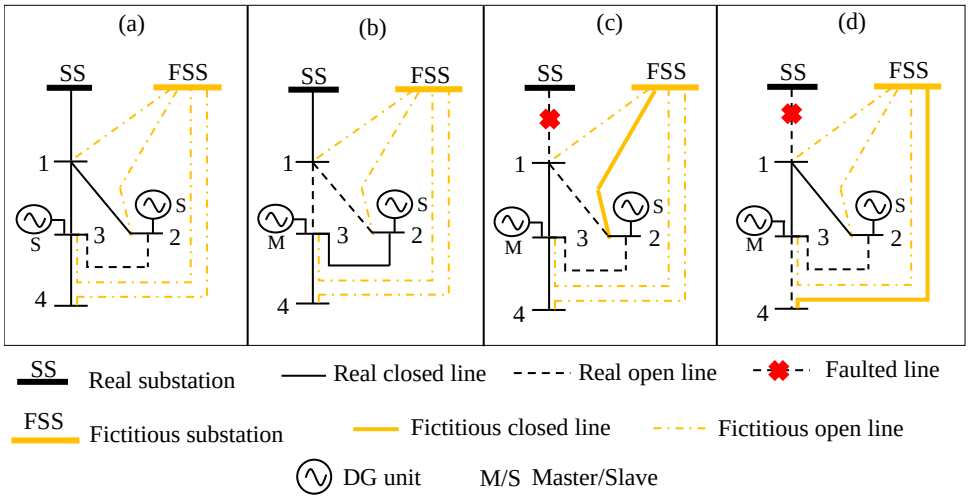

Figure 2: Islanding operation and restoration process

(31) for estimating the time that an MDG unit is connected at bus i. Constraint (32) is set to couple the binary variables that model the MDG units sent to new locations and the binary variables that estimate their connection time, z^{mgd} and w, respectively. Expression (33) ensures that once an MDG unit arrives and is installed at i, this unit remains available for the subsequent time periods. The available power of the MDG unit placed to i is defined by (34). The reactive power delivered by an MDG unit is controlled by (35). It worth noting that during emergency conditions, the DSO can send all the available MDG units to the new locations; however, in some cases, some MDG units may remain in their pre-defined staging locations.

2.5.3. Radiality constraints and islanding operation

In this approach, a fictitious grid is modeled to separate the in-service zone from the out-of-service zone of the EDS. This fictitious grid is composed by a fictitious substation connected to each node of the system. Besides, for islanding operation, a master-slave DG operation is considered in radial topology where large dispatchable DG units are considered as master units to be the voltage reference of its own islands while renewable and MDG units are considered as slaves [15].

For illustrative purposes, Fig. 2 presents a didactic four-bus and one substation system under different conditions. This figure also includes the fictitious grid. Fig. 2.a describes the normal operation of the system, in this situation, the DG units located at buses 2 and 3 are defined as slave units, all the nodes are in-service, and no connection with the fictitious substation (FSS) is required. For the condition presented in Fig. 2.b, the DG unit located at bus 3 is defined as a master unit and, thus, an island is formed with buses 2, 3, and 4. Meanwhile, bus 1 is feed by the substation (SS) and the DG unit at bus 2 was defined as a slave unit. Note that, in the situations show in Figs 2.a and 2.b, applying a fictitious grid was not necessary. In contrast, Fig. 2.c and .d, a fault at line $SS-1$ is analyzed. In these situations, the DG sited at bus 3 was defined as

the master unit while the DG unit at bus 2 as slave unit. In the situation presented by Fig. 2.c, an island is formed with buses 1, 3, and 4, while bus 2 is out-of-service, then, it must be connected to the fictitious substation FSS. In similar way, in Fig. 2.d, an island is formed with buses 1, 2, and 3, while the out-of-service bus 4 is connected to the fictitious substation.

$$F_{ij,f}^{SS} + F_{ji,f}^{SS} = y_{ij,f}, \qquad \forall (ij \in \Gamma_B \cup \Gamma_B^F, f \in \Gamma_F), \tag{36}$$

$$\sum_{ij \in \Gamma_B^*} F_{ij,f}^{SS} = 1, \qquad \forall (i \in \Gamma_N|_{i \notin \Gamma_S}, f \in \Gamma_F), \tag{37}$$

$$F_{ij,f}^{SS} = 0, \qquad \forall (ij \in \Gamma_B^*|_{i \in \Gamma_S}, f \in \Gamma_F). \tag{38}$$

The set of constraints (36)-(38) represents the radiality of the grid for each fault scenario f, avoiding the interconnection between substations and loop formation. The binary variable $y_{ij,f}$ determines the operational state of the line ij, if $y_{ij,f} = 1$ the line ij is closed for the fault scenario f, otherwise is open. Considering the substations buses as roots of a graph, the binary variable $F_{ij,f}^{SS}$ is used to determine the direction of the connection between buses. If $F_{ij,f}^{SS} = 1$, the buses i and j are connected in the direction $j \rightarrow i$. In this regard, if the line ij is closed constraint (36) determines the direction of connection between i and j. Note that this constraint also considers the fictitious grid. Disregarding the substation nodes, constraint (37) forces that all the nodes of the system must be connected by at less one line. To avoid the interconnection between two substation ($i \in \Gamma_S$), in constraint (38), variables $F_{ij,f}^{SS}$ that feed these buses are set to 0.

$$y_{ij,f} = \gamma_{j,f}^{m}, \qquad \forall (ij \in \Gamma_B, f \in \Gamma_F|_{i \in \Gamma_S \wedge j \in \Gamma_G}), \tag{39}$$

$$V_{j,t,c,f}^{sqr} = V^{dg^2}, \qquad \forall (j \in \Gamma_G, t \in \Gamma_T, c \in \Gamma_C^t|_{\gamma_{j,f}^m = 1}, f \in \Gamma_F). \tag{40}$$

For each fault scenario f, if a bus $j \in \Gamma_G$ is selected as a master unit, then the parameter $\gamma_{j,f}^{m}$ is set at 1. It means that this bus is denoted as a reference bus and cannot be connected with the EDS substations or with other master DG units. To do it, an extra substation is considered, this substation only has branches to connect with these DG units; however, the current capacity of these branches and the power capacity of this extra substation are null. If node j is selected as a master DG, constraint (39) forces its connection with the extra substation. Note that, constraints (39) and (38) avoid the interconnection between buses with master DG units since (38) avoids the interconnection between substations. The voltage at buses with a DG selected as a master unit is specified as V^{dg}, as shown in (40). It is worth mentioning that the master DG units are defined with large capacities and are selected before the optimization process according to each fault scenario f.

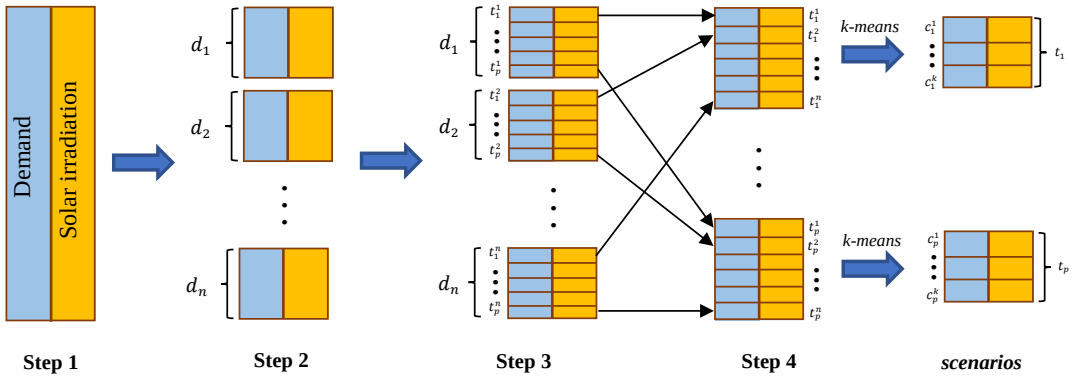

Figure 3: Scenario generation methodology

$$-(1-y_{ij,f}) \leq x_{i,f} - x_{j,f} \leq (1-y_{ij,f}), \qquad \forall (ij \in \Gamma_B, f \in \Gamma_F), \tag{41}$$

$$x_{j,f} \geq y_{ij,f}, \qquad \forall (ij \in \Gamma_H, f \in \Gamma_F). \tag{42}$$

An operating line can only connect buses with the same operational status. In this way, constraint (41) avoids the interconnection of in-service buses with non-restored buses, i.e., if $y_{ij,f} = 1$, then $x_{i,f} = x_{j,f}$, otherwise if $y_{ij,f} = 0$ then $x_{i,f}$ and $x_{j,f}$ are independent each other. Constraint (42) ensures that only out-of-service buses can be connected to the fictitious substation.

$$x_{i,f} = 0, \qquad \forall (i \in \Gamma_N^f, f \in \Gamma_F). \tag{43}$$

In a fault scenario f, the system's buses that were not affected by this fault must continue in-service after the restoration process, thus, constraint (43) fixes the load shedding variable $x_{i,f}$ at 0 in the set of load buses that were not affected by this fault.

2.6. Modeling uncertainty

In this approach, measurements of the load behavior and solar irradiation over a planning horizon are reduced to a set of stochastic scenarios using the k-means clustering technique as presented in Fig. 3. The methodology reduces a database of measurements according to time similarities to reproduce an operational day [33], as presented in the following steps:

- *Step 1:* Normalize the information dividing each value by its corresponding maximum measurement.
- *Step 2:* Considering that the database is chronologically ordered, separate the information into n days, as illustrated in Fig. 3, where each day is indicated as d_1, d_2, ... , d_n.
- *Step 3:* Define a number of periods (p) to discretize each day d. In Fig. 3, t_p^d represents the p-th period of the d-th day.

- *Step 4:* For each period, gather the data according to periods and use k-means to reduce it into a set of k clusters.

As presented in Fig. 3, the result is a set of stochastic scenarios that represent the horizon planning as a single day, where c_p^k indicates the k-th centroid of the cluster information contained in the p-th period. The probability ρ of each scenario is obtained by dividing the number of collected data in cluster c^k by the number of days n.

3. Case Studies

In this section, two distribution systems are used to validate the proposed approach under different test conditions. The two-stage stochastic MILP model was coded in AMPL and solved using CPLEX 20.1.0. The numerical experiments were processed on a computer with a 2.80 GHz Intel Core i7-7700 processor and 16 GB of RAM. The planning horizon, studied in this work, is 1 year. In this period, the uncertainty behavior of demand consumption and solar irradiation is captured through 24 stochastic scenarios that are obtained using the strategy proposed in section 2.6. This set of scenarios is generated considering characteristics of tropical countries from the information provided by [34]. It is worth mentioning that this set of scenarios are considered in both pre- and post-fault stages. To assess the performance of the presented approach against different emergency conditions, simultaneous fault scenarios at multiple circuits are taken into account. The fault scenarios are selected as high-impact and random due to the reduced repeatability of this type of event in the system.

3.1. 33-Node System

The proposed approach is tested using the 33-bus distribution system adapted from [30] and presented in Fig. 4, where all alternatives to be considered in the proposed approach are identified. For this system, it is considered that all the circuits have a switch. For quality requirements in this system, the lower and upper bounds of voltage magnitude are defined in 0.95 and 1.05 p.u., respectively. The system has three dispatchable DG units localized at buses 16 (1 MVA), 22 (1 MVA), and 29 (1.5 MVA). Two staging locations, S1 and S2, where each one can pre-positioned up to 5 MDG units of 0.20 MVA and a power factor of 0.8. These MDG units can dispatched and connected at buses 7, 12, 17, 22, 25, and 33. The requested traveling time (including congestion factor) by these units is presented in Fig. 4 and their connection time at bus i takes 1 hour. To assess the maximum penetration level of PV-based DG that can be accommodated in this system, buses 4, 8, 13, 18, 21, 26, and 28 were selected. In order to increase the connected PV-based DG capacity,

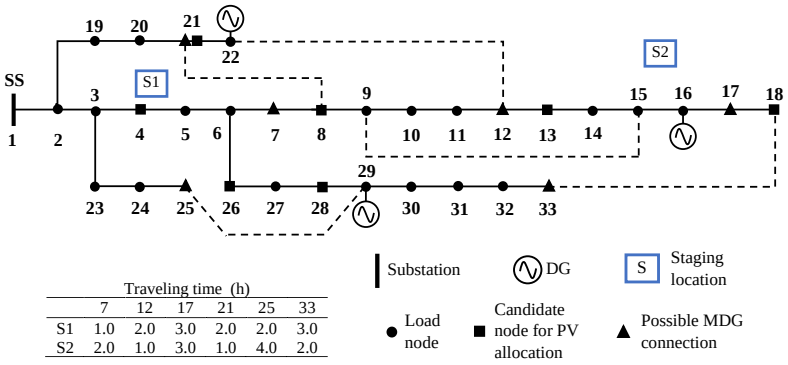

Traveling time (h)

	7	12	17	21	25	33
S1	1.0	2.0	3.0	2.0	2.0	3.0
S2	2.0	1.0	3.0	1.0	4.0	2.0

Figure 4: Pre-fault state of the 33-bus distribution system

Table 2: Studied Fault Scenarios and their impacts on the 33-Bus EDS

Fault Scen.	Faulted Circuits	Disconn. Demand	In-service Demand	Master DG units	Buses In-service
1	1-2, 6-7, 15-16, 20-21, 3-23, 24-25	100%	0	16, 22, 30	1
2	2-3, 7-8, 15-16, 24-25	87.62%	598 kW	16, 30	1, 2, 19, 20, 21, 22
3	3-4, 7-8, 15-16, 20-21, 3-23, 24-25	90.04%	481 kW	16, 22, 30	1, 2, 3, 19, 20

a maximum generation curtailment γ of 7% can be applied to overcome system limit violations. This value can be defined via contract between DG investors and DSO prior to solve the problem.

For each fault scenario, Table 2 presents the set of faulted circuits, the percent of demand that is affected by the fault, the demand that remains in-service after a fault scenario considering a load scenario of 1.0 p.u, the DG units that are selected as master units, and the load buses that remains in-service after the fault including the substation bus.

Under these fault scenarios, the proposed resilience-based strategy is studied considering different test conditions. These conditions are summarized in five cases presented as follows:

- Case I considers PV hosting capacity assessment and the dispatching problem of MDG units.
- For Case II, the PV hosting capacity assessment is disregarded. To attend emergency conditions, the dispatching of MDG units is considered.
- Case III considers the effects of estimating the PV hosting capacity without the dispatching of MDG units.
- In Case IV, PV hosting capacity and the dispatching of MDG units are disregarded.
- Case V is formulated as an analysis of two steps. In the first, the maximum penetration level of PV-based DG that can be accommodated in the EDS is estimated in normal conditions, in other words, no

fault scenario is analyzed. In the second step, the penetration level of PV-based DG, obtained in the first step, is fixed and by simulating the fault scenarios presented in Table 2, resilience-based strategies (reconfiguration, islanding operation and MDG units scheduling) are optimized.

It is worth mentioning that to minimize the negative impacts of the failure scenarios studied, the islanding operation with master-slave DG operation is considered for Cases I-IV.

Obtained results from Case I and Case II are summarized in Table 3. This table presents, after each fault scenario, the percent of demand in-service, the load buses that remains out-of-service, the disconnected and connected lines, and the dispatch of MDG units indicating their displacement ($Sx \rightarrow i$) and arrival time given in hours (xh). The CPU time was 19s and 10s, for cases I and II, respectively. Under conditions specified for Case I, only two MDG units were pre-positioned at the staging location $S1$ for attending emergency conditions due to the three fault scenarios. Considering the fault scenario 1, 77.66 % of demand is recovered by applying a restoration process. This process defines the islanding operation of three DG units, five sectionalizing switches must be open while three tie switches must be closed, and the MDG units are displaced to be connected at buses 7 and 3 with estimated arrival times of 2 and 3 hours, respectively. For the conditions studied in the fault scenario 2, after the restoration process, two buses remains out-of service and 83.31% of demand is recovered. The obtained solution defines the islanding operating mode to two DG units, located at buses 16 and 29, while the DG unit at bus 22 is operated as a slave unit connected to the substation bus SS, and the two MDG units are dispatched and connected simultaneously at bus 7 with an expected arrival time of 2 hours. Finally, under fault scenario 3, 80.89% is in-service, all the DG units are operating in islanding mode, and only one MGD unit is dispatched from $S1$ to be connected at bus 12 with arrival time of 3 hours. For this case, the entire restoration process is illustrated in Fig. 5, where for each fault scenario, all alternatives considered for service recovering are identified.

In Case II, the effects of estimating the maximum PV-based DG penetration level that can be accommodated in the EDS are disregarded. In analogous way, the restoration process allows restoring the same amount of demand that Case I. To achieve this goal, comparing with solutions of Case I, similar restoration actions are applied. However, three MDG units are required to be pre-positioned in the system, where two units are placed at staging location $S1$ while one unit at $S2$. This shows that the PV generation can influence the process, since more MDG units are required. The effects of the MDG units were analyzed on Case I and II. To validate the importance of this alternative, Cases III and IV are formulated disregarding the dispatch problem of MDG units. Solving these cases, the CPU time was 13s and 7s, respectively. Obtained results for these cases are presented in Table 4, where is indicated the percent of in-service demand, load buses

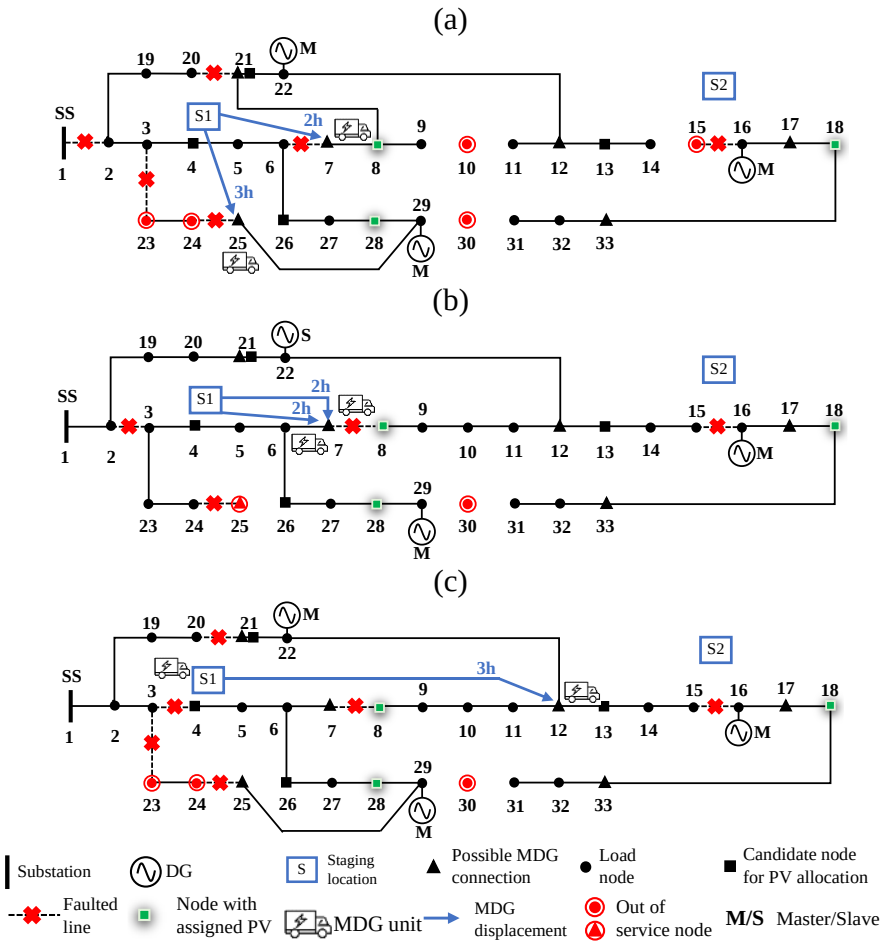

Figure 5: Post-fault state of the 33-bus EDS for Case I. (a) solution for fault scenario 1, (b) solution for fault scenario 2, (c) solution for fault scenario 3.

that remains out-of-service, and the disconnected and connected circuits of the EDS. It worth noting that comparing the total amount of in-service demand for both cases, this value is improved in 0.54 %, 0.54 %, and 3.23 % for each fault scenario when the PV hosting capacity is estimated in Case III. On the other hand, comparing numerical results obtained from Case I and Case III, the MDG units represent an increasing of 8.88 %, 4.84 % and 2.42 % on the amount of in-service demand. In similar way, comparing Case I and Case IV, the simultaneous optimization of MDG units and the estimation of the PV hosting capacity represent 9.42 %, 5.38 % and 5.65 % of improvements on the in-service demand.

In order to determine the effects of considering the PV hosting capacity on the resilience problem, Case V is studied. This case is based on two steps, the first one estimates the PV hosting capacity under normal conditions. Meanwhile, in the second step, the determined PV penetration level is fixed and by simulating the three fault scenarios, all the resilience alternatives are optimized. The solution of this case shows that, by comparing the estimated PV capacity found in Case I and II, increasing of 300.16% and 315.05% were achieved. However, to deal with infeasible conditions under fault scenarios and after the restoration problem,

Table 3: Restoration Process For Cases I and II - 33-Bus system

Case	Fault Scen.	Demand in-service	Faulted Buses	Open Circuits	Closed Circuits	MDG Dispatch
I	1	77.66%	10, 15, 23, 24, 30	9-10, 10-11, 14-15, 29-30, 30-31	8-21, 12-22, 18-33, 25-29	S1→7 (2h); S1→25 (3h)
	2	83.31%	25, 30	29-30, 30-31	12-22, 18-33	S1→7 (2h); S1→7 (2h)
	3	80.89%	23, 24, 30	29-30, 30-31	12-22, 18-33, 25-29	S1→12 (3h)
II	1	77.66%	09, 15, 23, 24, 30	8-9, 9-10, 14-15, 29-30, 30-31	8-21, 12-22, 18-33, 25-29	S1→25 (3h); S1→25 (3h); S2→12 (2h)
	2	83.31%	25, 30	29-30, 30-31	12-22, 18-33	S1→7 (2h); S1→7 (2h)
	3	80.89%	23, 24, 30	29-30, 30-31	12-22, 18-33, 25-29	S1→7 (2h); S2→12 (2h)

Table 4: Restoration Process For Cases III and IV - 33-Bus system

Case	Fault Scen.	Demand in-service	Faulted Buses	Open Circuits	Closed Circuits
III	1	68.78%	14, 15, 19, 20, 21, 23, 24, 30	13-14, 2-19, 21-22, 29-30, 30-31	12-22, 18-33, 25-29
	2	78.47%	3, 23, 24, 30	3-4, 29-30, 30-31	8-21, 18-33, 25-29
	3	78.47%	21, 23, 24, 30	21-22, 29-30, 30-31	12-22, 18-33, 25-29
IV	1	68.24%	7, 19, 20, 21, 23, 24, 30	7-8, 2-19, 21-22, 29-30, 30-31	12-22, 18-33, 25-29
	2	77.93%	7, 24, 30	6-7, 23-24, 29-30, 30-31	12-22, 18-33, 25-29
	3	75.24%	4, 21, 23, 24, 30	4-5, 21-22, 29-30, 30-31	12-22, 18-33, 25-29

the generation curtailment was of 80 %. This energy curtailment could cause economic damage for independent DG investors. In this regard, this fact evidences that the DG hosting capacity should be assessed in a simultaneous way with a restoration process. The detail information, for each bus, of the installed PV capacity and its generation curtailment, is summarized in Table 5.

3.2. Adapted 118-Node System

The scalability of the proposed approach is validated using the adapted 118-node system, obtained from [35] and presented in Fig. 6. For quality requirements, the lower and upper bounds of voltage magnitude are defined in 0.93 and 1.05 p.u., respectively. The system has four dispatchable DG units localized at buses 49 (2.5 MVA), 72 (2 MVA), 86 (2 MVA), and 110 (2 MVA). Two staging locations, S1 and S2, are defined in this system, where each one can accommodate up to 4 MDG units with a capacity of 0.25 MVA. Each MEG unit has a power factor of 0.8. These MDG units can be dispatched and connected at buses 26, 34, 59, 84,

Table 5: Installed PV Capacity and Energy Curtailment For Each Bus - 33-Bus system

Bus	Case I		Case III		Case V	
	Capacity (MW)	Curt. (MWh)	Capacity (MW)	Curt. (MWh)	Capacity (MW)	Curt. (MWh)
4	0.00	0.00	0.00	0.00	1.14	4.16
8	0.53	0.20	0.48	0.18	2.12	9.05
13	0.00	0.00	0.00	0.00	0.67	2.92
18	0.45	0.17	0.45	0.17	0.19	0.00
21	0.00	0.00	0.00	0.00	0.61	2.63
26	0.00	0.00	0.72	0.27	0.39	1.48
28	0.74	0.28	0.00	0.00	1.73	6.61
Total	1.72	0.65	1.65	0.63	6.87	26.85

Table 6: Studied Fault Scenarios and their impacts on the 118-bus EDS

Fault Scen.	Faulted Circuits	Disconn. Demand	In-service Demand	Master DG units
1	1-100	22.23%	17661.48 kW	110
2	1-100, 1-63	54.73%	10281.15 kW	72, 86, 110
3	1-63	32.50%	15329.39 kW	72, 86
4	1-2, 1-100	67.50%	7380.33 kW	49, 110
5	1-2, 1-63	77.77%	5048.24 kW	49, 72, 110
6	1-2	45.27%	12428.57 kW	49
7	1-2, 1-63, 1-100	100.00%	0.00	49, 72, 86, 110

and 109. For test purposes here, buses 9, 20, 41, 42, 62, 64, 71, 86, 87, and 108 were randomly selected as candidate locations to assess the PV-based DG hosting capacity. Note that the set of candidate nodes to install PV-based DG depends on the distribution company preferences and possibilities. For each PV-based DG, a maximum generation curtailment γ of 7% can be applied to overcome system limit violations under pre- and post- fault conditions.

For each fault scenario, Table 6 presents the set of faulted circuits, the percent of affected demand, the demand that remains in-service after each fault scenario considering a load scenario of 1.0 p.u, and the DG units that are selected as master units. To solve the restoration problem and reduce the search space in this problem, a tier 1 strategy is used, as presented in [36]. This strategy determines that only the switches incident to the out-of-service area can be switched to restore the system while the switches that do not incident with the out-of-service area are fixed in their initial status. In this case, the relative MIP gap tolerance for CPLEX MIP was set at 1.0%.

Under these fault scenarios, the proposed strategy is studied considering two test conditions, as follows:

- Case I considers PV hosting capacity assessment and the dispatching problem of MDG units.
- Case II is formulated as two steps analysis. In the first step, the maximum penetration level of PV-based DG that can be accommodated in the EDS is estimated in normal conditions. Then, in the second step, the fault scenarios presented in Table 6 are simulated and the optimization model is solved considering all the proposed resilience-based strategies. This case is similar to proposed case V for the 33-node system.

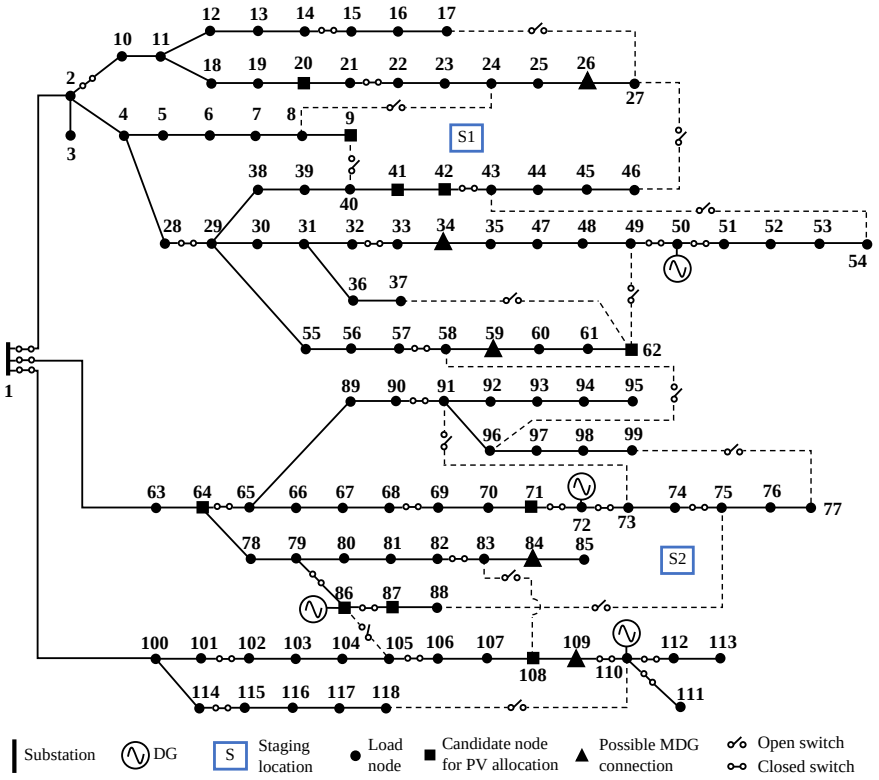

Figure 6: Pre-fault state of the 118-bus distribution system

For these cases the CPU time was 110000s and 317s, respectively. For Case I, the obtained results are presented in Table 7, where the percent range of in-service load after the restoration process is of 36.56 to 95.96% for fault scenarios 7 and 1, respectively.

Under the proposed fault scenarios, the obtained solution for case I indicates the pre-allocation of two MGD units at staging location S2. However, these units are not required to be dispatched in each fault scenario, results indicate that the MDG are dispatched only for fault scenarios 1, 4, 5, and 7. For illustrative purposes, Fig. 7 presents the locations where PV-based DG units were installed, the restored topology for the fault scenario 1 (fault at circuit 1-100), and the displacements of the MDG units. In this fault scenario, the restoration process proposes the islanding operation of the DG located at bus 110, while the other DG units operate in slave mode connected to the main grid. In addition, two MDG units are displaced from the staging location $S2$ to be connected to bus 109. After the implementation of these resilience alternatives, only the bus 111 remains out-of-service.

Table 8 shows the installed PV capacity and energy curtailment for Case I and Case II for each bus. In Case I, a total DG capacity of 8.55 MW was installed divided at buses 62, 71, 86, and 87. This solution determines that a total generation curtailment of 1.70 MWh should be implemented to attend operational constraints.

Table 7: Results of Restoration Process For Case I - 118-Bus EDS

Fault Scen.	Demand in-service	Open Circuits	Closed Circuits	MDG Dispatch
1	95.96%	101-102, 109-110, 110-111	105-86, 110-118	S2→109 (1h); S2→109 (1h)
2	75.88%	64-65, 72-73, 74-75, 79-86, 90-91, 101-102, 105-106, 109-110, 110-111	58-96, 88-75, 105-86, 110-118	-
3	90.73%	64-65, 72-73, 82-83, 79-86, 90-91	58-96, 88-75, 108-83	-
4	56.63%	32-33, 49-50, 57-58, 101-102, 109-110, 110-111	58-96, 105-86, 110-118	S2→109 (1h)
5	51.40%	32-33, 49-50, 57-58, 64-65, 72-73, 82-83, 79-86, 90-91	62-49, 58-96, 88-75, 108-83	S2→59 (2h)
6	60.67%	32-33, 49-50, 57-58	58-96	-
7	36.56%	32-33, 49-50, 57-58, 64-65, 72-73, 74-75, 79-86, 90-91, 101-102, 105-106, 109-110, 110-111	62-49, 58-96, 88-75, 105-86, 110-118	S2→34 (2h)

Table 8: Installed PV Capacity and Curtailment For 118-Bus EDS

Bus	Case I		Case II	
	Capacity (MW)	Curt. (MWh)	Capacity (MW)	Curt. (MWh)
9	0.00	0.00	1.74	4.95
20	0.00	0.00	4.03	11.45
41	0.00	0.00	4.49	12.74
42	0.00	0.00	1.16	3.30
62	3.12	0.62	3.47	1.23
64	0.00	0.00	5.79	16.44
71	2.94	0.58	3.79	2.28
86	0.65	0.13	3.14	2.01
87	1.84	0.37	0.11	0.00
108	0.00	0.00	5.77	16.38
Total	8.55	1.70	33.50	70.77

In Case II, the first step which disregards the fault scenarios determines a total installed capacity of 33.50 MW, which is around 390% bigger than in Case I. However, in the second step when fault scenarios are simulated, a generation curtailment above 80% is mandatory to maintain the EDS operation without technical violations. Therefore, these results validate the relevance of the DG hosting capacity analysis considering simultaneously normal and emergency conditions, since excessive generation curtailments can be applied when high-impact fault occur.

Finally, for comparative purposes, an additional test was conducted disregarding the PV hosting capacity analysis and the dispatch of MDG problem. Results show that the percent range of in-service load after the restoration process, varies from 33.79% to 90.12% in fault scenarios 1 and 7, respectively. These solutions have an in-service demand that is 2.77% and 5.84% lower when compared with the solutions obtained in case I for the same fault scenarios, presented in Table 7. Then, it is possible to verify that the resilience of the 118-bus system can be improved when the PV-based generation capacity to be installed and the dispatch of MDG units problem are simultaneously optimized.

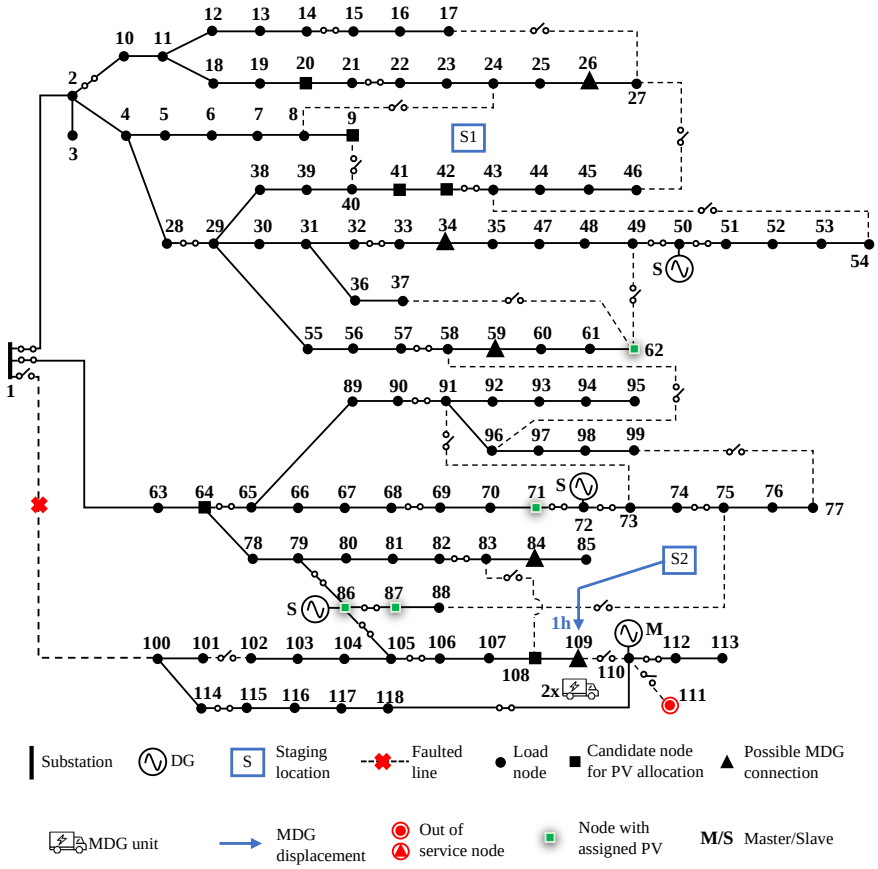

Figure 7: Post-fault state of the 118-bus system for the fault scenario 1

4. Discussion

Results demonstrate the effectiveness of the proposed approach to deal with simultaneous planning and restoring problems. The proposed mixed-integer linear programming model guarantees finite convergence using a commercial optimization solver. Numerical experiments show the effectiveness of the proposed approach to solving the 33 node distribution system, however, it is observed a notable increase in the CPU time solving the 118 node system. In this regard, the tier 1 strategy is an adequate alternative to solve the restoration problem in a large distribution system in an acceptable CPU time.

In both test systems, the optimal pre-positioning and dispatch of MDG units show benefits since increase the amount of restored energy in all fault scenarios. The PV hosting capacity of the systems is severely affected by the resilience approach. As presented in case V and case II, for the 33-node and 118-node systems, respectively, results indicate that installed PV capacity of the system could be 4 times higher when the resilience approach is disregarded. However, this high PV penetration requires a generation curtailment of up to 80% to attend the system under emergency conditions.

5. Conclusion

In this work, a strategy to improve the resilience of distribution systems after a set of fault scenarios has been formulated. To deal with emergency conditions and to improve the recoverability of the system, the islanding operation through a dynamic topology reconfiguration, master-slave operation scheme with dispatchable DG unis, and the dispatch problem of MDG units are optimized simultaneously. In addition, the proposed approach seek to estimate the maximum capacity of PV-based DG that can be installed in an EDS.

From the numerical results can be observed that by optimizing the dispatch of MDG units, the amount of restored demand can be increased when compared with solutions where this alternative was disregarded. The effects of estimating the maximum capacity of PV-based generation, simultaneously with the restoration process, show that the number of pre-positioned and dispatched MDG units can be reduced when compared with a case where the integration of PV-based DG is not considered. Nevertheless, when the PV-based generation capacity is maximized under normal conditions without taking into account any fault scenarios, this value can reach more than 300%. This increase in the PV-based generation leads to unviable operational conditions during fault scenarios and high power generation curtailments are required to deal with such conditions. In this regard, from an economic point of view, this curtailment could cause negative impacts for independent DG investors. Therefore, this fact evidences that there is a high risk if a greater DG hosting capacity is adopted disregarding the resilience studies. Finally, when PV hosting capacity and the dispatch problem of MDG units are simultaneously optimized, results demonstrate that the EDS resilience can be improved. Future work will address further advances in the formulation, for example considering risk-based analysis to determine the most suitable solution, where negative impacts on the benefits of DG developers are mitigated even with the occurrence of high-impact events.

Acknowledgment

This work was supported by the São Paulo Research Foundation (FAPESP) under Grants 2019/01841-5, 2019/23755-3, 2018/12422-0 and 2015/21972-6, CAPES under Finance Code 001, and CNPq under Grant 304726/2020-6. J.P.S. Catalão acknowledges the support by FEDER funds through COMPETE 2020 and by Portuguese funds through FCT, under POCI-01-0145-FEDER-029803 (02/SAICT/2017).

References

[1] M. Panteli and P. Mancarella, "The grid: Stronger, bigger, smarter?: Presenting a conceptual framework of power system resilience," *IEEE Power and Energy Magazine*, vol. 13, no. 3, pp. 58–66, 2015.

[2] M. A. Mohamed, T. Chen, W. Su, and T. Jin, "Proactive resilience of power systems against natural disasters: A literature review," *IEEE Access*, vol. 7, pp. 163 778–163 795, 2019.

[3] P. Hallberg *et al.*, "Active distribution system management a key tool for the smooth integration of distributed generation," *Eurelectric TF Active System Management*, vol. 2, no. 13, 2013.

[4] S. M. Ismael, S. H. A. Aleem, A. Y. Abdelaziz, and A. F. Zobaa, "State-of-the-art of hosting capacity in modern power systems with distributed generation," *Renew. energy*, vol. 130, pp. 1002–1020, 2019.

[5] O. D. Melgar-Dominguez, D. A. Quijano, J. R. S. Mantovani, and G. Chicco, "A Robust Multiobjective Strategy for Short-Term Distribution System Upgrading to Increase the Distributed Generation Hosting Capacity," *IEEE Transactions on Power Systems*, vol. To be published, pp. 1–1, 2022.

[6] A. Almalaq, K. Alqunun, M. M. Refaat, A. Farah, F. Benabdallah, Z. M. Ali, and S. H. A. Aleem, "Towards Increasing Hosting Capacity of Modern Power Systems through Generation and Transmission Expansion Planning," *Sustainability*, vol. 14, no. 5, p. 2998, 2022.

[7] M. Mahzarnia, M. P. Moghaddam, P. T. Baboli, and P. Siano, "A review of the measures to enhance power systems resilience," *IEEE Systems Journal*, vol. 14, no. 3, pp. 4059–4070, 2020.

[8] M. Panteli, D. N. Trakas, P. Mancarella, and N. D. Hatziargyriou, "Power systems resilience assessment: Hardening and smart operational enhancement strategies," *Proceedings of the IEEE*, vol. 105, no. 7, pp. 1202–1213, 2017.

[9] Y. Lin and Z. Bie, "Tri-level optimal hardening plan for a resilient distribution system considering reconfiguration and dg islanding," *Applied Energy*, vol. 210, pp. 1266–1279, 2018.

[10] K. S. A. Sedzro, A. J. Lamadrid, and L. F. Zuluaga, "Allocation of resources using a microgrid formation approach for resilient electric grids," *IEEE Trans. Power Systems*, vol. 33, no. 3, pp. 2633–2643, 2018.

[11] J. M. Home-Ortiz and J. R. S. Mantovani, "Resilience enhancing through microgrids formation and distributed generation allocation," in *2020 IEEE PES Innovative Smart Grid Technologies Europe (ISGT-Europe)*. IEEE, 2020, pp. 995–999.

[12] G. Zhang, F. Zhang, X. Zhang, Q. Wu, and K. Meng, "A multi-disaster-scenario distributionally robust planning model for enhancing the resilience of distribution systems," *International Journal of Electrical Power & Energy Systems*, vol. 122, p. 106161, 2020.

[13] A. Shahbazi, J. Aghaei, S. Pirouzi, T. Niknam, M. Shafie-khah, and J. P. Catalão, "Effects of resilience-oriented design on distribution networks operation planning," *Electric Power Systems Research*, vol. 191, p. 106902, 2021.

[14] Z. Wang and J. Wang, "Self-healing resilient distribution systems based on sectionalization into microgrids," *IEEE Trans. Power Syst.*, vol. 30, no. 6, pp. 3139–3149, 2015.

[15] T. Ding, Y. Lin, Z. Bie, and C. Chen, "A resilient microgrid formation strategy for load restoration considering master-slave distributed generators and topology reconfiguration," *Applied energy*, vol. 199, pp. 205–216, 2017.

[16] B. Chen, C. Chen, J. Wang, and K. L. Butler-Purry, "Multi-time step service restoration for advanced distribution systems and microgrids," *IEEE Trans. Smart Grid*, vol. 9, no. 6, pp. 6793–6805, 2018.

[17] S. Lei, C. Chen, Y. Li, and Y. Hou, "Resilient disaster recovery logistics of distribution systems: Co-optimize service restoration with repair crew and mobile power source dispatch," *IEEE Trans. Smart Grid*, vol. 10, no. 6, pp. 6187–6202, 2019.

[18] B. Taheri, A. Safdarian, M. Moeini-Aghtaie, and M. Lehtonen, "Distribution system resilience enhancement via mobile emergency generators," *IEEE Trans. Power Delivery*, 2020.

[19] L. F. Ochoa, C. J. Dent, and G. P. Harrison, "Distribution network capacity assessment: Variable dg and active networks," *IEEE Transactions on Power Systems*, vol. 25, no. 1, pp. 87–95, 2010.

[20] Z. M. Ali, I. M. Diaaeldin, S. HE Abdel Aleem, A. El-Rafei, A. Y. Abdelaziz, and F. Jurado, "Scenario-based network reconfiguration and renewable energy resources integration in large-scale distribution systems considering parameters uncertainty," *Mathematics*, vol. 9, no. 1, p. 26, 2020.

[21] S. F. Santos, D. Z. Fitiwi, M. Shafie-Khah, A. W. Bizuayehu, C. M. Cabrita, and J. P. Catalão, "New multistage and stochastic mathematical model for maximizing res hosting capacity—part i: Problem formulation," *IEEE Trans. Sustai. Energy*, vol. 8, no. 1, pp. 304–319, 2017.

[22] D. Liu, C. Wang, F. Tang, and Y. Zhou, "Probabilistic assessment of hybrid wind-pv hosting capacity in distribution systems," *Sustainability*, vol. 12, no. 6, p. 2183, 2020.

[23] O. D. Melgar-Dominguez, J. R. S. Mantovani, M. Pourakbari-Kasmaei, and M. Lehtonen, "Increasing distributed generation hosting capacity in distribution networks: A co2 emission analysis," in *2020 IEEE PES Innovative Smart Grid Technologies Europe (ISGT-Europe)*, 2020, pp. 1010–1014.

[24] R. Cadenovic and D. Jakus, "Maximization of distribution network hosting capacity through optimal grid reconfiguration and distributed generation capacity allocation/control," *Energies*, vol. 13, no. 20, 2020.

[25] D. A. Quijano, O. D. Melgar-Dominguez, C. Sabillon, B. Venkatesh, and A. Padilha-Feltrin, "Increasing distributed generation hosting capacity in distribution systems via optimal coordination of electric vehicle aggregators," *IET Gener. Transmiss. & Distrib.*, vol. 15, no. 2, 2021.

[26] S. M. Ismael, S. H. Abdel Aleem, A. Y. Abdelaziz, and A. F. Zobaa, "Probabilistic hosting capacity enhancement in non-sinusoidal power distribution systems using a hybrid PSOGSA optimization algorithm," *Energies*, vol. 12, no. 6, p. 1018, 2019.

[27] M. Rawa, A. Abusorrah, Y. Al-Turki, S. Mekhilef, M. H. Mostafa, Z. M. Ali, and S. H. Aleem, "Optimal allocation and economic analysis of battery energy storage systems: Self-consumption rate and hosting capacity enhancement for microgrids with high renewable penetration," *Sustainability*, vol. 12, no. 23, p. 10144, 2020.

[28] Z. M. Ali, I. M. Diaaeldin, A. El-Rafei, H. M. Hasanien, S. H. A. Aleem, and A. Y. Abdelaziz, "A novel distributed generation planning algorithm via graphically-based network reconfiguration and soft open points placement using Archimedes optimization algorithm," *Ain Shams Engineering Journal*, vol. 12, no. 2, pp. 1923–1941, 2021.

[29] J. R. Birge and F. Louveaux, *Introduction to stochastic programming*, 2nd ed. New York: Springer, 2011.

[30] M. E. Baran and F. F. Wu, "Network reconfiguration in distribution systems for loss reduction and load balancing," *IEEE Power Engineering Review*, vol. 9, no. 4, pp. 101–102, 1989.

[31] N. Alguacil, A. L. Motto, and A. J. Conejo, "Transmission expansion planning: a mixed-integer lp approach," *IEEE Transactions on Power Systems*, vol. 18, no. 3, pp. 1070–1077, 2003.

[32] S. Lei, J. Wang, C. Chen, and Y. Hou, "Mobile emergency generator pre-positioning and real-time allocation for resilient response to natural disasters," *IEEE Trans. Smart Grid*, vol. 9, no. 3, pp. 2030–2041, 2018.

[33] J. M. Home-Ortiz and J. R. S. Mantovani, "Enhancement of the resilience through microgrids formation and dg allocation with master-slave dg operation," in *2020 International Conference on Smart Energy Systems and Technologies (SEST)*. IEEE, 2020, pp. 1–6.

[34] I. Staffell and S. Pfenninger, "Renewables. ninja," 2018.

[35] D. Zhang, Z. Fu, and L. Zhang, "An improved ts algorithm for loss-minimum reconfiguration in large-scale distribution systems," *Electric Power Systems Research*, vol. 77, no. 5-6, pp. 685–694, 2007.

[36] Karen Nan Miu, Hsiao-Dong Chiang, and R. McNulty, "Multi-tier service restoration through network reconfiguration and capacitor control for large-scale radial distribution networks," *IEEE Transactions on Power Systems*, vol. 15, no. 3, pp. 1001–1007, 2000.